

MATHEMATICAL BIOLOGY: SOME OPPORTUNITIES IN INTEGRATIVE BIOLOGY

R. MEJIA

*NHLBI, National Institutes of Health
10 Center Drive, Room B1D416
Bethesda, MD 20892-1061 USA
E-Mail: ray@helix.nih.gov*

Integrative Biology is the study of an organism within a framework in an integrated, systematic manner in order to discern governing principles or mechanisms. Quantitative tools applied in the study of biological organisms include, in addition to statistical analyzes and hypothesis testing, mathematical modeling. Computational tools used include databases to organize both the data and models into a form that is linked and readily usable. I will describe mathematical models integrated into research in physiology as well as tools being developed by the Physiome Project with the support of the International Union of Physiological Sciences. The goal of the Physiome Project is the quantitative description of the integrated function of living organisms, and for the human physiome, to develop quantitative biology to improve medical science from genes to health. The “model validate” cycle used in Mathematical Biology is iterated to refine our understanding of the biology as illustrated here with experiments, databases and modeling in kidney physiology.

1. Introduction

Models have been used to study biological processes at varying space and time scales from DNA to RNA, proteins, pathways, networks, cells, tissues and organs. In DNA analysis whole-genome shotgun sequencing was initially considered unworkable, but was predicted to be feasible by statistical analysis [57]. Since then it has been used to sequence the human genome [56, 25] as well as other genomes [16]. RNA molecules with pseudo-knots have been analyzed mathematically [15], and models have been used to predict the outcome of small interfering RNA (siRNA) therapy in the treatment of cancer [1]. Protein folding has been a fertile field of study. Monte Carlo models of protein folding abound, for example, in dynamic Monte Carlo simulation of helix-coil transition [8]. Gene networks and regulatory pathways of the cell cycle in yeast and bacteria have been elu-

culated using mathematical models by Tyson and coworkers [54, 38, 5] for two decades. Recently, quantitative models have described biochemical networks in signal transduction, metabolic pathways and regulatory networks as described in [6]. At the cellular level, mathematical models have contributed to the understanding of the function of many cell types such as pancreatic beta cells [4], kidney cells [30, 58], and smooth muscle cells [34, 22, 59]. Modeling at the tissue level has contributed to the understanding of disease progression such as in cancer [51, 31]. At the organ level, models have played an important role in cardiac physiology, specifically in the study of the pacemaker [55] and cardiac dynamics [23, 46]. More broadly still, the Cardiome Project has sought to describe the functioning heart [2, 3]. Currently synthetic biology is beginning to make it possible to design and study new organisms [44].

The Human Physiome Project of the International Union of Physiological Sciences (IUPS) has as goal the quantitative description of the integrated functions of living organisms, and seeks to develop quantitative biology to improve medical science from genes to health [20, 19]. This goal has also been undertaken by the EuroPhysiome initiative [13, 52]. Integral to this effort is the development of databases to organize and disseminate data to both bench scientists and modelers. This is supported by the development and use of markup languages that facilitate the exchange of data and models across compute platforms. Markup languages in use include SBML [18] for representation of biochemical reaction networks, CellML [29] for description of mathematical models of cellular function, and MorphML [11] for description of neuroanatomical data, coding and sharing information.

An active area of investigation in renal physiology has been the study of the mechanism by which the mammalian kidney produces a concentrated urine. Mathematical models have contributed to the understanding of processes involved in the physiology and pathophysiology of the kidney since Stephenson [48, 49] and Kokko and Rector [24] first described the kidney as a countercurrent exchanger and multiplier. The kidney physiome project, promulgated by Schafer [47] and others [20, 53] under the auspices of the IUPS, seeks to integrate tools for use in renal physiology. We describe how bench scientists and modelers are collaborating to use techniques of molecular biology and imaging to refine mathematical models of the mammalian kidney, and how the physiome project seeks to facilitate the exchange of physiological data and models.

2. Model of the Kidney

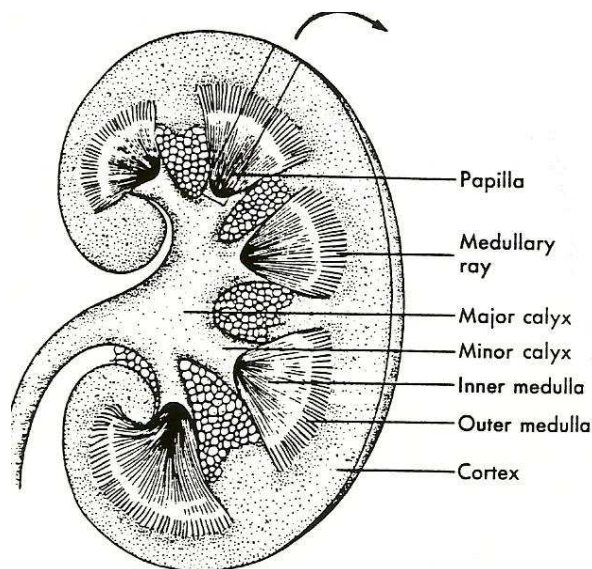


Figure 1. A schematic diagram of a cross section of the human kidney. The rectangular section (top of figure) delineates nephro-vascular units in the cortex and the medulla that are modeled.

The mammalian kidney serves to maintain homeostasis by excreting impurities, byproducts of diet and metabolism, and conserving water and other solutes necessary for body function. A schematic diagram of a cross section of the human kidney (Figure 1) shows multiple papillae that contain nephro-vascular units. Small solutes and water are filtered from arterial blood by glomerulii in the cortical region and travel through nephron segments that are permselectable. The fluid that reaches the nephron's terminal segment, the collecting duct, flows into a calyx at the bottom of the papilla and is excreted through the ureter. Blood vessels in each pyramid exchange water and solutes with the nephrons and return reabsorbate to the venous circulation. A mathematical model of a water and solute movement in a single nephro-vascular population was first described by Stephenson and coworkers [50]. A model with populations of short and long nephrons is shown schematically in Figure 2. This model shows transport of water, NaCl, and urea to and from nephron segments and the vasculature through

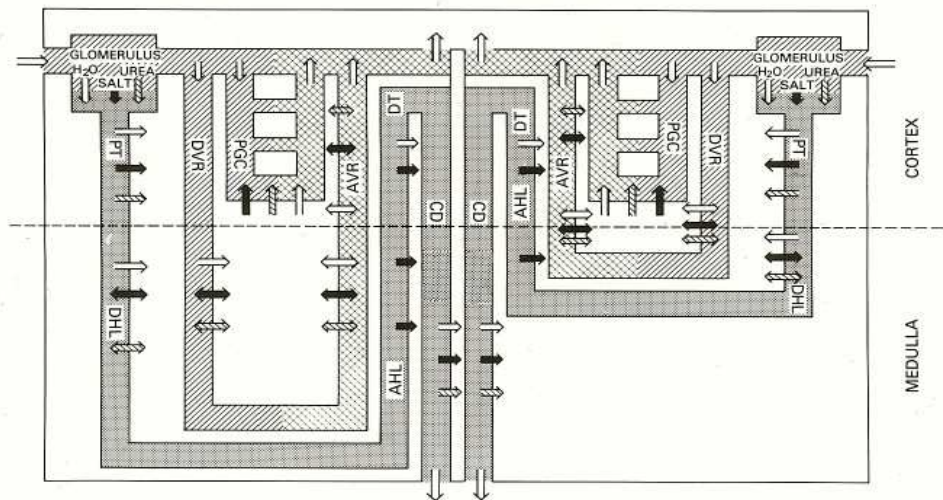


Figure 2. A schematic diagram of a model with two nephro-vascular units. Water and solute movement is shown with water (clear arrow), NaCl (black arrow), urea (stippled arrow). Segments are: proximal tubule (PT), descending Henle's limb (DHL), ascending limb of Henle (AHL), distal tubule (DT), collecting duct (CD), descending vas rectum (DVR), ascending vas rectum (AVR) and post-glomerular capillary (PGC).

an interstitial space.

2.1. Actions of Atrial Natriuretic Factor

A model where the interstitium and vasa recta are merged into a single compartment, the central core, is shown in Figure 3. The model has five populations of short and long nephrons that account for 71, 13, 9, 5 and 2% of nephrons in the rat kidney, respectively. This model has been used to study three hypothetical steady-state effects of atrial natriuretic factor (ANF) on the concentrating mechanism [35]: namely, inhibition of NaCl absorption in the collecting duct, inhibition of water permeability in the collecting duct, and increased glomerular filtration rate.

Table 1 shows the composition of fluid at three locations in the nephron: the outflow from the distal cortical tubule, the flow into the cortical collecting duct, and the outflow from the collecting duct. The composition in the control, a rat kidney with arginine vasopressin stimulated collecting duct water permeability, is compared with the composition for (*i*) reduced

$V_{m,CCD}^{NaCl}$, (ii) reduced $P_{f,IMCDt}$, and (iii) increased delivery of fluid to the proximal straight tubule $V_{PST}(0)$ that represents increased GFR in the model. Boundary values and other model parameters are given in [35].

Table 1 shows that the three actions of ANF considered have little effect on urea as shown by the fraction of filtered load excreted. Inhibition of NaCl absorption in the cortical collecting duct by reduction of $V_{m,CCD}^{NaCl}$ by 50 and 90% increased NaCl delivery to the IMCDt (not shown) and NaCl excretion. Water excretion also increased as predicted. Inhibition of water permeability in the terminal segment of the inner medullary collecting duct

Table 1. Composition for Control and Hypothesized Actions of ANF

| | Water | | NaCl | | Urea | | Total Osmolality, mosmol/kgH ₂ O |
|------------------------|-----------|-----------|-----------|----------|-----------|----------|---|
| | FFL x 100 | V, nl/min | FFL x 100 | Conc, mM | FFL x 100 | Conc, mM | |
| Control | | | | | | | |
| DCT out | 19.74 | 4.94 | 6.11 | 46 | 55.4 | 18 | 130 |
| CCD in | 9.59 | 2.40 | 5.37 | 84 | 149.1 | 101 | 311 |
| CD out | 0.96 | 0.24 | 0.27 | 42 | 46.9 | 318 | 822 |
| 50% $V_{m,CCD}^{NaCl}$ | | | | | | | |
| DCT out | 19.66 | 4.92 | 6.08 | 46 | 55.4 | 18 | 130 |
| CCD in | 9.17 | 2.29 | 5.30 | 87 | 130.8 | 93 | 309 |
| CD out | 1.14 | 0.28 | 0.84 | 111 | 46.7 | 266 | 835 |
| 10% $V_{m,CCD}^{NaCl}$ | | | | | | | |
| DCT out | 19.64 | 4.91 | 6.08 | 46 | 55.4 | 18 | 130 |
| CCD in | 8.89 | 2.22 | 5.26 | 89 | 117.9 | 86 | 308 |
| CD out | 1.32 | 0.33 | 1.41 | 159 | 46.7 | 229 | 843 |
| 50% $P_{f,IMCDt}$ | | | | | | | |
| DCT out | 19.58 | 4.89 | 6.06 | 46 | 55.4 | 18 | 130 |
| CCD in | 9.20 | 2.30 | 5.24 | 86 | 137.2 | 97 | 311 |
| CD out | 1.02 | 0.26 | 0.20 | 29 | 46.9 | 299 | 745 |
| 20% $P_{f,IMCDt}$ | | | | | | | |
| DCT out | 19.34 | 4.83 | 5.98 | 46 | 55.4 | 19 | 131 |
| CCD in | 8.60 | 2.15 | 5.05 | 88 | 118.7 | 90 | 310 |
| CD out | 1.12 | 0.28 | 0.11 | 15 | 47.0 | 272 | 643 |
| 1.025 $V_{PST}(0)$ | | | | | | | |
| DCT out | 20.29 | 5.20 | 6.83 | 50 | 55.4 | 18 | 137 |
| CCD in | 10.01 | 2.57 | 6.04 | 90 | 126.9 | 82 | 305 |
| CD out | 1.23 | 0.32 | 0.89 | 108 | 47.1 | 248 | 800 |
| 1.05 $V_{PST}(0)$ | | | | | | | |
| DCT out | 20.92 | 5.49 | 7.57 | 54 | 55.4 | 17 | 144 |
| CCD in | 10.58 | 2.78 | 6.75 | 96 | 110.1 | 68 | 299 |
| CD out | 1.57 | 0.41 | 1.64 | 156 | 47.3 | 196 | 778 |

FFL is fraction of filtered load.

Flow rate (V) in the collecting duct is normalized by the total number of glomerulotubular units in rat kidney (38,000).

Therefore, to obtain total flow in the collecting duct, values are multiplied by 38,000.

DCT values are for short nephrons only. See the text for definition of other parameters.

by reduction of $P_{f,IMCDc}$ by 50 and 80% increased water excretion slightly, and NaCl excretion was reduced slightly relative to the control. The major effect was a reduction in urine osmolality due to incomplete equilibration with the medullary interstitium or central core. Increased flow to the proximal straight tubule, $V_{PST}(0)$, results in increased NaCl and water delivery to the distal cortical tubule, increased NaCl and water excretion, and urinary NaCl concentration close to the plasma concentration (150 mM). A 2.5 and 5% increase in $V_{PST}(0)$ increased delivery to the distal cortical tubule of superficial nephrons by over 5 and 11% respectively.

The results support the conclusion that the overall effect of an increase in circulating ANF is due to multiple actions of ANF in the kidney that result in a more effective regulatory response than a single action could produce.

2.2. Synergy of Models and Experiments

A curated database of renal parameter (RPDB) for use by modelers has been implemented by Legato et al. [27]. It includes experimental conditions for measurements with links to the literature and to regulatory and transporter proteins. Measurement of water and solute transport in segments of the rat loop of Henle has not been reported. However, a query to RPDB for “chinchilla” shows permeabilities measured for several segments of the descending and ascending thin limb [9, 10], as does a search for “hamster” [21]. Hence, permeabilities of the loop of Henle in the rat have been extrapolated from measurements made in other rodents. These measurements have been made using tubule perfusion [7]. A segment of tubule is dissected and mounted on an apparatus such that the composition of the perfusate and of the solution bathing the tubule is known. The composition of the outflow at the distal end of the tubule is used to calculate the transport. However, perfusion does not resolve the question of changes in transport within the segment of tubule perfused, where uniform transport is generally assumed. Immunofluorescent immunolabeling [40, 37], on the other hand, has been used to identify transporters expressed in individual portions of a tubule. Antibodies to a protein are conjugated with a fluorophore in order to label a transporter in the cells that form a tubule.

Models have described quantitatively the mammalian urine concentration mechanism. They have shown that the permselectability of the nephron segments produces gradients for water and solute transport in the

medulla. However, none has shown how the kidney produces the solute gradient in the inner medulla that is necessary to produce a concentrated urine. Immunolabeling has also shown that nephron segments and the vasculature are located preferentially in the medulla. This suggests that the solute composition of the interstitium is not homogeneous at a given depth. Instead, tubules that extend to the same depth may be exposed to different osmotic gradients in the surrounding interstitium.

Experiments by Pannabecker et al. [40] in rat, mouse and rabbit have shown that in the inner medulla descending thin limbs of Henle (DTL) and ascending thin limbs of Henle (ATL) express different transporters in adjacent segments. They have also shown that DTL segments may be permeable to water, NaCl, or urea, while an ATL segment may be permeable to NaCl or urea. Mejia and Wade [37] have shown that in the rat inner medulla more thin limbs (TL) of Henle were labeled by antibodies to chloride channel marker ClC-K1 than by antibodies to water channel marker AQP1 (Table 2). This suggests that some DTL segments transport NaCl and not water. In addition, TL were labeled by ClC-K1 on both sides of the hairpin turns, showing that DTL shift from expressing AQP1 to expressing ClC-K1 at some distance from where they turn and begin to ascend. Since AQP1 is expressed in vasa recta (VR) as well as in DTL, von Willebrand Factor (vWF) and morphology (the diameter of VR is greater than that of DTL) were used to obtain the estimate of DTL shown in Table 2.

Table 2. Sprague-Dawley rat tubules labeled and estimates of DTL and ATL

| Distance to Tip μm | Labeled by <i>ClC</i> (<i>ATL</i>) | Labeled by <i>AQP1</i> (<i>DTL</i>) | Estimated <i>ATL</i> ¹ Incidence | % <i>DTL</i> with <i>AQP1</i> | Incidence <i>ClC</i> labeled <i>DTL</i> |
|--|--|---|---|-------------------------------------|---|
| 50 (4) ² | 74± 25 | 16 ± 1 ³ | 45± 13 | 36 | 29± 12 |
| 50 (2) ² strong <i>ClC</i> | 60± 2 | 16 ± 1 ³ | 38± 1 | 43 | 22± 1 |
| 100 (3) ² | 83± 15 | 12 ± 2 ³ | 48± 8 | 26 | 35± 6 |
| 100 (3) ² strong <i>ClC</i> | 37± 10 | 12 ± 2 ³ | 24± 6 | 50 | 12± 5 |
| 200 (3) ² | 99± 4 | 19 ± 8 ⁴ | 59± 5 | 32 | 40± 5 |
| Junction IM-OM (2) ² | 190± 33 | 72± 21 | 131± 27 | 55 | 59± 6 |

¹ (*AQP1* + *ClC*)/2
²(n) is average for n sections at this depth
³ *DTL* labeled by *AQP1* = structures labeled by *AQP1* – VR estimated from adjacent sections
⁴ *DTL* labeled by *AQP1* = structures labeled by *AQP1* – structures labeled by vWF as VR

Layton and coworkers [26] have used data about the three dimensional structure of the outer medulla to group the nephrovascular segments into four groups, each with its own interstitium [26, Figure 1]. The three dimen-

sional architecture of the rat inner medulla has been described by Dantzler and coworkers [39, 41, 42], and a model has been used to compute sodium and urea concentration profiles and osmolality in the inner medulla [43, Figures 2 and 3]. It remains to test these observations with a model of the whole kidney.

3. Kidney Physiome

Effort undertaken by the Physiome Project [20] has resulted in the construction of a repository for models written in CellML [29]. The EuroPhysiome Project supports access to several databases for use by investigators including the Quantitative Kidney Database (QKDB) [12]. QKDB links to several renal databases and other resources. The databases include the Collecting Duct Database of regulatory and transporter proteins (CDDB) [28], the Collecting Duct Phosphoprotein Database (CDPD) [17], and the Urinary Exosome Protein Database [45] that contains protein products identified in the urine and facilitates a BLAST [32] comparison of an amino acid sequence against the database.

4. Summary

We have described how a study of the urine concentration mechanism of the mammalian kidney has used methods in experimental physiology, molecular biology, bioinformatics and mathematical modeling. This is a multidisciplinary effort - the type that the Physiome Project seeks to stimulate, and is representative of the many opportunities available for contribution by mathematical biologists in the full breadth of research, from the genome to the organism.

5. Appendix

5.1. Model Equations

A multinephron model of the mammalian kidney described by Mejia, et al. [35] has been used to study the urine concentrating mechanism. The model combines the vasculature and interstitium into a central core [49], and is described as follows:

$$\begin{aligned}\partial_t(AC) + \partial_x \mathbf{F} &= -\mathbf{J}, \\ \partial_t A + \partial_x F_v &= -J_v, \\ \partial_x P &= -R_v F_v,\end{aligned}\tag{1}$$

where mass flow is given by

$$\mathbf{F} = F_v \mathbf{C} - A(\mathbf{D} \partial_x \mathbf{C});$$

x is distance along the cortico-papillary axis; t is time; A is the cross-sectional area of the segment; \mathbf{C} is a vector of solute concentrations; F_v is volume flow; \mathbf{J} is solute flux (positive defined to be out of the lumen). J_v is volume flux out of the lumen. P is hydrostatic pressure; R_v is resistance to flow, and \mathbf{D} are solute diffusion coefficients.

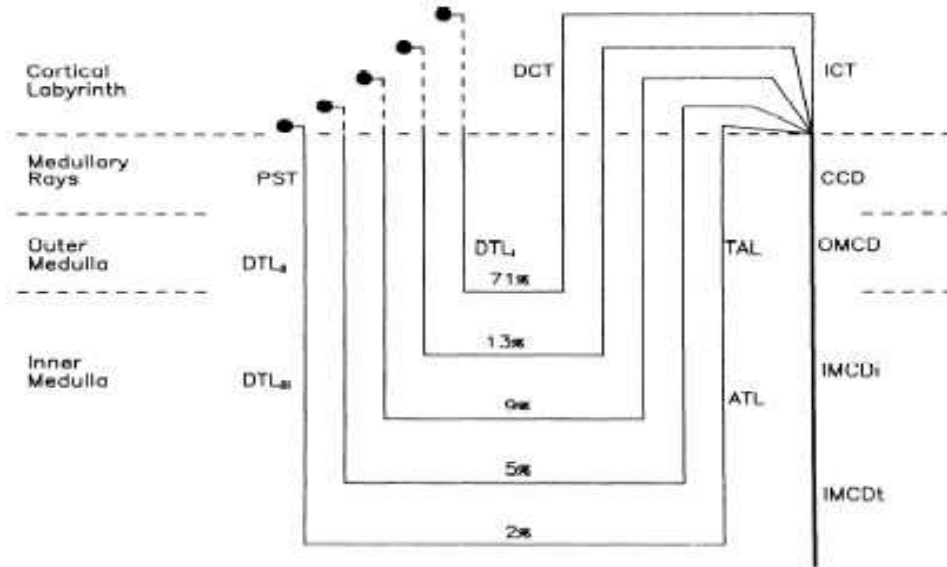


Figure 3. A schematic diagram of central core model with five nephron populations. The nephron segments are: proximal straight tubule (PST), short descending thin limb of Henle (DTL_I), long descending thin limb (DTL_{II} , DTL_{III}), distal cortical tubule (DCT), thick ascending thick limb (TAL), ascending thin limb (ATL), initial collecting tubule (ICT), cortical collecting duct (CCD), outer medullary collecting duct (OMCD) and inner medullary collecting duct (IMCDi, IMCDt). In the rat 71% are short nephrons, while 2% extend to the papilla.

Transmural water flux is given by

$$J_v = -2\pi\rho P_f V_w \sum_k \sigma_k \Delta C_k,$$

where ρ is the radius of the tubule; P_f is the water permeability; V_w is the partial molar volume of water; σ_k is the reflection coefficient of the k^{th}

species, and $\Delta C_k = C_k - C_{Ck}$, where C_k and C_{Ck} are the concentration of the k^{th} species in the lumen and central core, respectively.

Transmural solute flux is given by

$$J_k = 2\pi\rho P_k \Delta C_k + (1 - \sigma_k) \underline{C}_k J_v + J_k^a,$$

where P_k is the solute permeability of the k^{th} species, and $\underline{C}_k = (C_k + C_{Ck})/2$. Active transport of the k^{th} species is given by

$$J_k^a = \frac{V_{mk} C_k}{K_{mk} + C_k},$$

where V_{mk} is the maximum rate of active transport, and K_{mk} is the Michaelis constant.

Water and mass conservation require that

$$J_{Cv}(x) = - \sum_i J_{iv}(x),$$

$$J_{Ck}(x) = - \sum_i J_{ik}(x),$$

where subscript C represents the medullary central core, and summation is over all tube segments i that extend to medullary depth x .

In the cortex, the interstitium is considered to be a well-mixed compartment with the concentration of each solute equal to that of plasma (superscript p), so that

$$\mathbf{C} = \mathbf{C}^p,$$

and the hydrostatic pressure is prescribed as

$$P_c = P_c^o.$$

The central core is treated as a tube open at the border of the cortical labyrinth and the medullary rays and closed at the papilla. Thus equations (1) hold, and boundary conditions for $t \geq 0$ are

$$A_C(L) \partial_t \mathbf{C}_C(L, t) = \mathbf{C}_C(L, t) J_{Cv}(L, t) - \mathbf{J}_C(L, t),$$

$$F_{Cv}(L, t) = \mathbf{F}_C(L, t) = 0,$$

$$P_C(0, t) = P_c^o,$$

where L is the depth of the medulla. Boundary conditions for each nephron population are given by

$$\mathbf{C}_1(0, t) = \mathbf{C}_1^0, \quad F_{1v}(0, t) = F_{1v}^0,$$

$$P_\ell(L, t) = P_b,$$

where subscripts 1 and ℓ refer to the first and last tube segment of each nephron population, respectively, and P_b is the bladder pressure. Intermediate boundary data are obtained by matching the value entering a tube segment to that leaving the previous segment (Figure 3).

Initial conditions at each axial position x and time $t = 0$ in the lumen and central core are given by

$$\mathbf{C}(x, 0) = \mathbf{C}^0, \quad F_v(x, 0) = F_v^0, \quad P(x, 0) = P^0.$$

5.2. Solution Method

Whole kidney multinephron models are non-linear multi-point boundary value problems. A partitioning scheme described in [36] has been used to reduce the storage and computation time, and a second-order implicit numerical scheme is used to discretize the differential equations [36]. Multiple steady-state solutions may exist, so we have used a parameter continuation scheme described in [33] to solve the discretized equations. An implementation of the continuation algorithm is available at <ftp://ftp.ncifcrf.gov/pub/users/mejia/ray/conkub.tar.Z>.

Accounting for multiplicity of solutions is required when computing the transition from one steady-state to another. This is illustrated for transition from diuresis to antidiuresis in [33, Figure 7].

References

1. J. C. Arceiro, T. L. Jackson, and D. E. Kirschner, *DCDS* **4**, 39 (2004).
2. J. B. Bassingthwaighite, *Adv. Exp. Med. Biol.* **382**, 331 (1995).
3. J. B. Bassingthwaighite, *Adv. Exp. Med. Biol.* **430**, 325 (1997).
4. R. Bertram, A. Sherman, and L. S. Satin, *Am. J. Physiol. Endocrinol. Metab.* **293**, E890 (2007).
5. P. Brazhnik, and J. J. Tyson, *Cell Cycle* **5**, 522 (2006).
6. R. Breitling, D. Gilbert, M. Heiner, and R. Orton, *Brief Bioinform.* **9**, 404 (2008).
7. M. Burg, J. Grantham, M. Abramow, and J. Orloff, *Am. J. Physiol.* **210**, 1293 (1966).
8. Y. Chen, Y. Zhou, and J. Ding, *Proteins* **69**, 58 (2007).
9. C. L. Chou, and M. A. Knepper, *Am. J. Physiol.* **263**, F417 (1992).
10. C. L. Chou, and M. A. Knepper, *Am. J. Physiol.* **264**, F337 (1993).
11. S. Crook, P. Gleeson, F. Howell, J. Svitak, R. A. Silver, *Neuroinformatics* **5**, Summer 96 (2007).

12. V. Dzodic, S. Hervy, D. Fritsch, H. Khalfallah, M. Thereau, and S. R. Thomas, *Cell Mol. Biol. (Noisy-le-grand)* **50**, 795 (2004). See <http://physiome.ibisc.fr/qkdb/>.
13. J. W. Fenner, et al., *Philos. Transact. A Math. Phys. Eng. Sci.* **366**, 2979 (2008).
14. P. A. Gonzales, et al., *J. Am. Soc. Nephrol. (in press)*
15. C. Haslinger, and P. F. Stadler. *Bull. Math. Biol.* **61**, 437 (1999).
16. H. Herlyn, and H. Zischler, *Genome Dyn.* **2**, 17 (2006).
17. J. D. Hoffert, G. Wang, T. Pisitkun, R. F. Shen, and M. A. Knepper, *J. Proteome Res.* **6**, 3501 (2007). See <http://dir.nhlbi.nih.gov/papers/lkem/cdpd/>.
18. M. Hucka et al., *Bioinformatics* **19**, 524 (2003).
19. P. J. Hunter, E. J. Crampin, and P. M. Nielsen, *Brief. Bioinform.* **9**, 333 (2008).
20. P. Hunter, P. Robbins, and D. Noble, *Pflugers Arch.* **445**, 1 (2002). See <http://www.physiome.org.nz/index.html>.
21. M. Imai, J. Taniguchi, and K. Yoshitomi, *Am. J. Physiol.* **254**, F323 (1988).
22. A. Kapela, A. Bezerianos, N. M. Tsoukias, *J. Theor. Biol.* **253**, 238 (2008).
23. J. P. Keener, *J. Cardiovasc. Electrophysiol.* **14**, 1225 (2003).
24. J. P. Kokko, and F. C. Rector Jr, *Kidney Int.* **2**, 214 (1972).
25. E. S. Lander, et al., *Nature* **409**, 860 (2001).
26. A. T. Layton, and H. E. Layton, *Am. J. Physiol. Renal Physiol.* **289**, F1346 (2005).
27. J. Legato, M. A. Knepper and R. Mejia, <http://cddb.nhlbi.nih.gov/rpdb/>, unpublished.
28. J. Legato, M. A. Knepper, R. A. Star, and R. Mejia, *Physiol. Genomics* **13**, 179 (2003). See <http://cddb.nhlbi.nih.gov/cddb/>.
29. C. M. Lloyd, M. D. Halstead, and P. F. Nielsen, *Prog. Biophys. Mol. Biol.* **85**, 433 (2004). See <http://www.physiome.org.nz/index.html>.
30. R. M. Lynch, R. Mejia and R. S. Balaban, *Comments Mol. Cell Biophys.* **5**, (1988), 151.
31. B. P. Marchant, J. Norbury, and H. M. Byrne, *Math. Med. Biol.* **23**, 173 (2006).
32. S. McGinnis, and T. L. Madden, *Nucleic Acids Res.* **32**, W20 (2004). See <http://blast.ncbi.nlm.nih.gov/Blast.cgi>.
33. R. Mejia, *J. Comput. Phys.* **63**, 67 (1986).
34. R. Mejia and R. M. Lynch, BIOMAT 2006 International Symposium on Mathematical and Computational Biology, Mondaini, R.P. and Dilão, R. (Eds) (2007), ISBN 978-981-270-768-0.
35. R. Mejia, J. M. Sands, J. L. Stephenson, and M. A. Knepper, *Am. J. Physiol.* **257**, F1146 (1989).
36. R. Mejia and J. L. Stephenson, *J. Comput. Phys.* **32**, 235 (1979).
37. R. Mejia and J. B. Wade, *Am. J. Physiol. Renal Physiol.* **288**, F553 (2002).
38. B. Novák, and J. J. Tyson, *Biochem. Soc. Trans.* **31**, 1526 (2003).
39. T. L. Pannabecker, D. E. Abbott, and W. H. Dantzler, *Am. J. Physiol. Renal Physiol.* **286**, F38 (2004).
40. T. L. Pannabecker, A. Dahlmann, O. H. Brokl, and W. H. Dantzler, *Am. J.*

- Physiol. Renal Physiol.* **278**, F202 (2000).
41. T. L. Pannabecker, and W. H. Dantzler, *Am. J. Physiol. Renal Physiol.* **287**, F767 (2004).
 42. T. L. Pannabecker, and W. H. Dantzler, *Am. J. Physiol. Renal Physiol.* **293**, F696 (2007).
 43. T. L. Pannabecker, W. H. Dantzler, H. E. Layton, and A. T. Layton, *Am. J. Physiol.* **295**, F1271 (2008).
 44. Peccoud J, et al., *PLoS ONE*. **3**, e2671 (2008).
 45. T. Pisitkun, R. F. Shen, and M. A. Knepper, *Proc. Natl. Acad. Sci. USA* **101**, 1336 (2004). See <http://dir.nhlbi.nih.gov/papers/lkem/exosome/>.
 46. J. J. Rice, M. S. Jafri, and R. L. Winslow, *Am. J. Physiol. Heart Circ. Physiol.* **278**, H913 (2000).
 47. J. A. Schafer, *Ann. Biomed. Eng.* **28**, 1002 (2000).
 48. J. L. Stephenson, *Nature* **206**, 1215 (1965).
 49. J. L. Stephenson, *Kidney Int.* **2**, 85 (1972).
 50. J. L. Stephenson, R. Mejia, and R. P. Tewarson, *Proc. Natl. Acad. Sci. USA*. **73**, 252 (1976).
 51. K. R. Swanson, C. Bridge, J. D. Murray, and E. C. Alvord Jr, *J. Neurol. Sci.* **216**, 1 (2003).
 52. S. R. Thomas, Wiley Interdisciplinary Reviews Systems Biology, in press.
 53. S. R. Thomas, et al., *Philos. Transact. A Math. Phys. Eng. Sci.* **366**, 3175 (2008).
 54. J. Tyson, *Proc. Natl. Acad. Sci. USA* **88**, 7328 (1991).
 55. A. Varghese, and R. L. Winslow, *J. Theor. Biol.* **168**, 407 (1994).
 56. J. C. Venter, et al., *Science* **291**, 1394 (2001).
 57. J. L. Weber, and E. W. Myers, *Genome Res.* **7**, 401 (1997).
 58. A. M. Weinstein, *Am. J. Physiol. Renal Physiol.* **280**, F1072 (2001).
 59. P. F. Zhuk, S. A. Karakhim, V. F. Gorchev, and S. A. Kosterin, *Ukr. Biokhim. Zh.* **80**, 123 (2008).